

A STATISTICAL DESCRIPTION OF SUPERSONIC JET MIXING NOISE*

Christophe Bailly†

Laboratoire de Mécanique des Fluides et d'Acoustique,
Ecole Centrale de Lyon, BP 163, 69131 Ecully cedex, France.

Abstract

This paper examines some recent developments in the modeling of supersonic jet noise using a compressible $k - \epsilon$ turbulence closure. To be more precise, we seek to improve predictions of high speed jet noise, e.g. in aerospace applications, by introducing CFD solutions for mean flow field properties into existing analytical models of aerodynamic noise. Three models of jet mixing noise are investigated in this study. First, the classical Lighthill's theory of aerodynamic noise is combined with Ribner's modeling of the source term. The usual Gaussian time correlation is replaced by a new function to improve low frequency predictions. The second approach relies on the Goldstein & Howes convected wave equation, which is here used to improve the prediction of mixing noise in the upstream direction. Then an original third model based on Ffowcs Williams & Maidanik's analysis is reviewed. In this model, only the Mach wave noise component is evaluated when the convection Mach number is supersonic. These three models are applied to shock-free high-speed round jets. Comparisons to experimental data, in particular for sound source localization, show good qualitative agreement.

Nomenclature

A	constant to simplify the notations, $A = \rho_j^2 / (\rho_o 16 \pi^2 c_o^5)$,
c	sound speed,
C	convection or Doppler factor,
D	exit nozzle diameter,
D_θ	directivity of the shear-noise, $D_\theta = (\cos^4 \theta + \cos^2 \theta) / 2$,
k	turbulent kinetic energy $k = 3u'^2 / 2$,
L	turbulence longitudinal length scale,
M_c	convection Mach number, $M_c = U_c / c_o$,
St	Strouhal number $St = fD / U_j$,

U_{axis}	local center-line velocity,
U_c	local convection velocity,
U_j	jet exit velocity,
u'	turbulence velocity scale $u'^2 = 2k/3$,
x	observer position,
y	local source point,
ϵ	dissipation rate of k ,
ρ	density,
τ_t	turbulence time scale,
ω	angular frequency
ω_t	turbulence angular frequency.

subscripts

0	in the homogeneous medium at rest,
1	in the axial direction,
2	in the radial direction.

1. Introduction

It has been known for a long time that gaseous jets generate noise. Since the work of Lighthill¹ classical jet theory² has been developed in terms of turbulent velocity fluctuations in a source term of a wave equation, or more recently in terms of large scale instabilities to predict in particular the broadband shock noise.³ Progress in computational fluid dynamics also allows new strategies for the calculation of acoustic fields radiated by turbulent flows.^{4,5} At least three approaches may be distinguished,⁶ each including a variety of methods for the representation of the flow, the acoustic sources and the radiated sound. The first class of methods relies on a numerical solution of the full compressible Navier-Stokes equations. Very large computing facilities are required to solve for the turbulence and the radiated acoustic field, but the generation and propagation of sound are directly calculated. In the second group of methods the acoustic far field is evaluated in two steps through an acoustic analogy and a turbulence model. The inner turbulent field can be obtained from a large eddy simulation or by synthesizing the fluctuating velocity field from knowledge of the mean flow. The acoustic far field is then deduced by solv-

*Copyright © 1997 by the American Institute of Aeronautics and Astronautics, Inc. All rights reserved.

†Assistant Professor, Member AIAA

ing a wave equation via an integral formulation^{7,8} or by solving the linearized Euler equations.⁹ In the third group of methods the turbulent flow field is known only by statistical quantities such as k , the turbulent kinetic energy, and ϵ , its dissipation rate.

The goal of this paper is to describe some recent developments and applications of the last group of methods to supersonic jet noise. More precisely, although theories are now well known it seems interesting to combine these results with available numerical fluid dynamics tools to predict high speed jet noise when parametric studies are required. Thus, for example, the ratio of the secondary and primary exit velocities that minimizes the radiated acoustic power can be numerically determined¹⁰ for subsonic coaxial jets. A similar approach is developed by Khavaran^{11,12} to predict elliptic jet noise, for instance.

The paper is organized into three parts. Section 2 is devoted to a review of jet noise modeling using a $k - \epsilon$ turbulence closure. Finally, an application of the numerical predictions in terms of sound source localization is carried out in section 3.

2. Jet noise modeling

One of the most elaborate statistical source model applicable to jet noise is due to Ribner.¹³ This approach yields good subsonic jet mixing noise predictions when data provided by a $k - \epsilon$ turbulence closure are introduced into the model.^{14,10} Since our goal is to develop predictive models, it is important to note at once that a global and unique adjustable factor is needed in these models, and that this factor is adjusted based on a single comparison with an experimental point. This factor is then kept constant and used for all Mach numbers and all flow configurations (subsonic or supersonic round jets and coaxial jets). This source modeling is briefly reviewed in section 2, and in the present work the classical Gaussian time correlation¹³ is replaced by a new function to improve low frequency predictions. This approach has been extended to supersonic jet mixing noise.^{15,14} The comparison of predicted results with experimental data shows a good agreement in the first quadrant ($0 \leq \theta \leq 90^\circ$), see Figure 1 for the notations. However the comparison is less satisfactory in the second quadrant ($90^\circ \leq \theta \leq 180^\circ$), and the difference between calculations and measurements increases with the nominal Mach number.

The problem of obtaining accurate predictions in the upstream direction was pointed out previously by Goldstein & Howes,¹⁶ who derived a con-

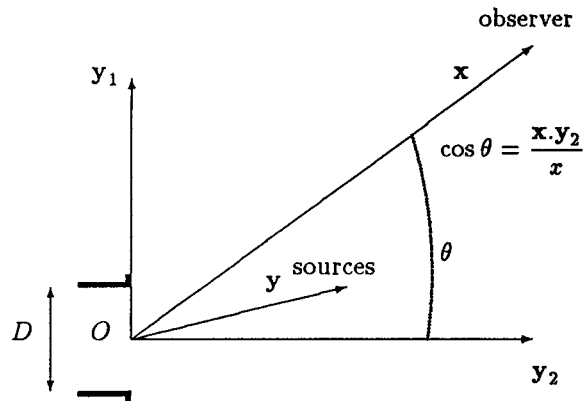


Figure 1: Sketch of the geometry.

vected wave equation for the pressure fluctuation. The main result of their analysis is a modification of the exponent -5 in the Doppler or convection factor, which is replaced by the exponent -3. A simple comparison of the equivalent power law with measurements shows a better agreement when using the -3 exponent, see Figure 2. An original contribution of the present study is to use a statistical description of the turbulent fluctuations in combination with this acoustic analogy to improve supersonic mixing noise prediction. One of the motivations for improving predictions in the upstream direction is to study acoustic effects during the launching of space vehicle systems. Indeed, although the radiated energy is higher for $0^\circ \leq \theta \leq 90^\circ$, acoustic energy radiated for $\theta \geq 90^\circ$ directly affects vehicle components. Following the same line of reasoning, the Mach wave noise component¹⁸ can be evaluated by following an analytical development of Ffowcs Williams & Maidanik.¹⁹ This model has been applied to a $M = 2$ supersonic round jet to predict the spectral peak as a function of the observer angle θ .

2.1 Aerodynamic results

The aerodynamic fields are obtained from a numerical solution of the Favre averaged Navier-Stokes equations with a compressible $k - \epsilon$ turbulence closure. These calculations are carried out with an axisymmetric compressible version of the ESTET code developed by Electricité de France. The effect that compressibility has on turbulence is taken into account through an energy dissipation resulting from dilatation processes. A description of the code and comparisons between numerical solutions and avail-

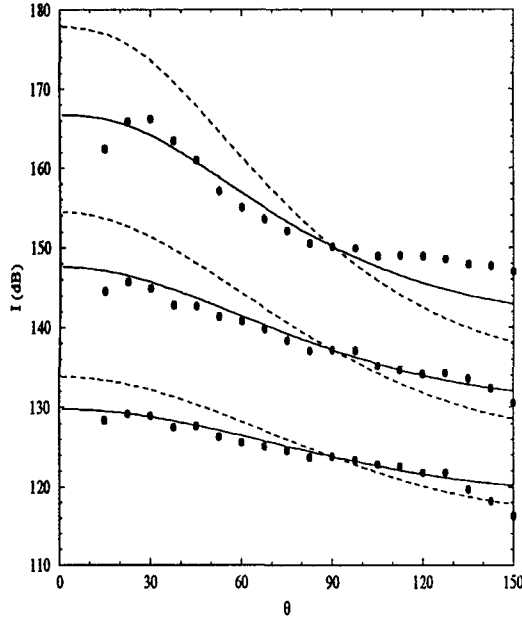


Figure 2: Jet directivity for three Mach number $M = 0.56$, $M = 0.86$ and $M = 1.33$. Power law: — Doppler factor at the power -3, - - - - Doppler factor at the power -5 (Lighthill's theory). • experimental data of Tanna¹⁷ *et al.*

able experimental data are provided in the literature.^{14,18} With knowledge of the mean velocity, the turbulent kinetic energy k and its dissipation rate ϵ , the turbulence time scale and the angular frequency are computed respectively, as $\tau_t \sim k/\epsilon$ and $\omega_t \sim 2\pi\epsilon/k$. The integral length scale is provided by $L \sim k^{3/2}/\epsilon$. Finally we approximate the convection velocity U_c to be constant in a transverse section of the jet and to be equal to a fraction of the local axial velocity: $U_c = 2/3U_{axis}$.

2.2 Modeling based on Ribner's theory

In the absence of solid boundaries, the integral solution of Lighthill's equation allows calculation of the autocorrelation function R_a of the far field acoustic fluctuations. To separate the effects of steady convection from the source term, a frame moving with this convection velocity $U_c \mathbf{y}_1$ is introduced, and

the function R_a per unit source volume becomes¹³:

$$R_a(\mathbf{x}|\mathbf{y}, \tau) = \frac{A}{x^2 C^5} \frac{\partial^4}{\partial \tau^4} \int_V R_{1111} d\xi \quad (1)$$

$$- \frac{A}{x^2 C^5} D_\theta \left(\frac{dU_1}{dy_2} \right)^2 \frac{\partial^4}{\partial \tau^4} \int_V \xi_2^2 R_{11} d\xi$$

where $A = \rho_j^2 / (\rho_o 16\pi^2 c_o^5)$ and D_θ is the directivity of the shear-noise (defined in the nomenclature). The Doppler or convection factor C is given by²⁰:

$$C(M_c, \theta) = \left[(1 - M_c \cos \theta)^2 + \left(\frac{\omega_t L}{\sqrt{\pi}} U_c \right)^2 \right]^{1/2}$$

where L is the integral longitudinal length scale and ω_t the turbulence angular frequency.

The fourth-order space-time velocity correlation function R_{1111} is expressed in terms of a sum of second-order correlations by assuming a normal distribution²¹:

$$\overline{u_1 u_1 u_1' u_1'} = 2\overline{u_1 u_1'} \overline{u_1 u_1'} + \overline{u_1 u_1} \overline{u_1' u_1'}$$

where only the first term contributes in (1). A separation of space-time variables is then assumed for the second-order correlation tensor $R_{11} = R(\xi)g(\tau)$, and the space factor for an isotropic turbulence is given by:

$$R(\xi) = u'^2 \left[\left(f + \frac{1}{2} \xi \frac{df}{d\xi} \right) \delta_{ij} - \frac{1}{2} \frac{df}{d\xi} \frac{\xi_i \xi_j}{\xi} \right]$$

The longitudinal correlation function is taken to be $f(\xi) = \exp(-\pi\xi^2/L^2)$ where L is the longitudinal integral turbulence length scale. Usually a Gaussian time correlation function $g(\tau)$ is chosen.^{13,14} As pointed out by Ribner,¹³ to calculate the power spectral density and the acoustic intensity given by $I(\mathbf{x}) = R_a(\mathbf{x}, \tau = 0)$ the two following quantities must be defined: $d^4 g/d\tau^4$ and $d^4 g^2/d\tau^4$ at $\tau = 0$. In this paper the Gaussian correlation is replaced by the following function to improve the low frequency predictions:

$$g(\tau) = \frac{1}{\cosh(\beta\omega_t \tau)} \quad (2)$$

where $\beta = 2/5$ is adjusted to fit the experimental data of Davies,²² see Figure 3.

A Fourier transform of the autocorrelation function (1) leads to the acoustic power spectral density S_a :

$$S_a(\mathbf{x}, \omega) = \int_V (S_a^{sj} + S_a^{sh}) dy \quad (3)$$

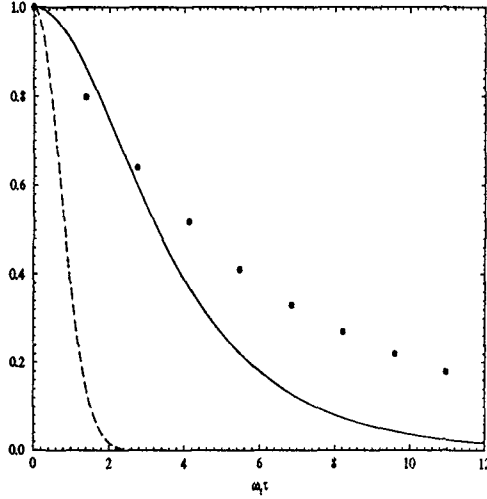


Figure 3: Modeling of the time correlation function. — hyperbolic function $g(\tau) = 1/\cosh(\beta\omega_t\tau)$, ---- Gaussian correlation $g(\tau) = \exp(-\tau^2\omega_t^2)$ and • data of Davies²² *et al.*

where the two components, namely the self-noise and the shear-noise, are given by:

$$S_a^{sf} = \frac{\rho_j^2 L^3 u'^4}{32\sqrt{2}\pi^2 \rho_o c_o^5 x^2} \frac{\omega^4}{\omega_t} \frac{1}{\beta\pi} \frac{\frac{\pi}{2\beta} \frac{C\omega}{\omega_t}}{\sinh\left(\frac{\pi}{2\beta} \frac{C\omega}{\omega_t}\right)} \quad (4)$$

$$S_a^{sh} = \frac{\rho_j^2 L^5 u'^2 D_\theta}{32\pi^3 \rho_o c_o^5 x^2} \left(\frac{dU_1}{dy_2}\right)^2 \frac{\omega^4}{\omega_t} \frac{1}{2\beta} \frac{1}{\cosh\left(\frac{\pi}{2\beta} \frac{C\omega}{\omega_t}\right)}$$

These expressions are very attractive because they allow sound source localization; an example is given in the next section. The total acoustic intensity is deduced by integrating the power spectral density (3) over all angular frequencies, or by taking the autocorrelation function (1) at $\tau = 0$:

$$I(\mathbf{x}) = \frac{\rho_j^2 L^3 u'^4}{32\sqrt{2}\pi^2 \rho_o c_o^5 C^5 x^2} \frac{d^4 g}{d\tau^4} \Big|_{\tau=0} + \frac{\rho_j^2 L^5 u'^2}{32\pi^3 \rho_o c_o^5 C^5 x^2} D_\theta \left(\frac{dU_1}{dy_2}\right)^2 \frac{d^4 g^2}{d\tau^4} \Big|_{\tau=0} \quad (5)$$

The influence of the time correlation function $g(\tau)$ on the spectra predictions is shown in Figure 4. The hyperbolic correlation (2) improves the low

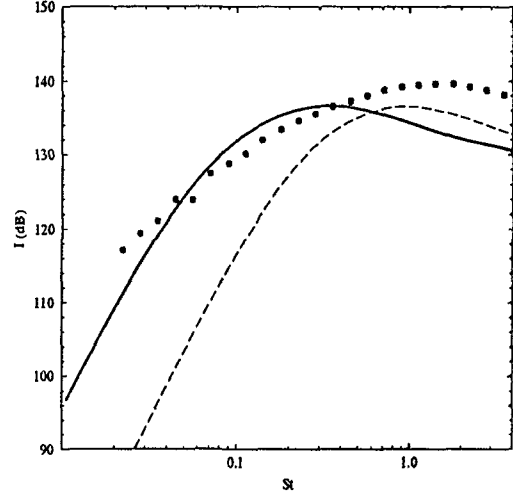


Figure 4: Influence of the time correlation function $g(\tau)$ on the spectrum. Third octave band spectra of a $M = 1.34$ round jet at $\theta = 90^\circ$. — hyperbolic correlation, ---- Gaussian correlation and • data of Tamia¹⁷ *et al.*

frequency predictions. A better numerical fitting of Davies data could be obtained for the correlation function. However to ensure convergence of the integral expression (3) we keep the hyperbolic correlation (2) in Ribner's model. The predictions underestimate the acoustic intensity for high frequencies or Strouhal numbers. This lack of accuracy could be attributed to the aerodynamic calculations.

2.3 Modeling based on Goldstein & Howes' theory

The convected wave equation of Goldstein & Howes¹⁶ is an alternative approach for improving the predictions of supersonic mixing noise. The starting point of this aerodynamic noise theory is the Lilley equation, which is reformulated so that the previous modeling of turbulence correlations can be applied to the source term. In their work¹⁶ the proposed integral solution is valid in the low frequency range with the result that refraction effects are neglected. Finally an expression of the autocorrelation of the acoustic far field fluctuations is obtained:

$$R_a(\mathbf{x}|\mathbf{y}, \tau) = \frac{A}{x^2 C^3} \frac{\partial^4}{\partial \tau^4} \int_V R_{1111} d\xi \quad (6)$$

$$- \frac{16}{3} \frac{A}{x^2 C^3} D_\theta \left(\frac{dU_1}{dy_2} \right)^2 \frac{\partial^4}{\partial \tau^4} \int_V \xi_2^2 R_{11} d\xi$$

Modeling of the source terms can be performed as in the previous section, which leads to an expression equivalent to (1) for the autocorrelation function. A subsequent Fourier transform yields to the acoustic power spectral density.²³ In this paper only the acoustic directivity is considered to show improvement in comparison with Ribner's results and measurements. For a Gaussian time correlation the acoustic intensity takes the following form:

$$I(\mathbf{x}) = \frac{1}{\pi^3 \rho_o c_o^5 x^2} \quad (7)$$

$$\times \int_V \frac{\rho^2 \overline{u'^2} L^3 \omega_i^4}{C^3} \left\{ \frac{3\overline{u'^2}}{2\sqrt{2}} + \frac{L^2}{\pi} \left(\frac{\partial U}{\partial y_2} \right)^2 D_\theta \right\} dy$$

This expression is very similar to the one derived via Ribner's theory except for the convection factor C , which appears now to the power -3. To illustrate this angular behaviour, the acoustic directivity of a $M = 1.33$ free jet is displayed in Figure 5 and is compared to Ribner's model and the experimental data of Tanna.¹⁷ The predictions are more accurate with Goldstein & Howes' model, particularly in the upstream direction.

2.4 A Mach wave noise model

When turbulent structures are convected supersonically relative to the ambient speed of sound, i.e. $M_c = U_c/c_o > 1$, the acoustic field radiated by this non-compact turbulent volume source is very efficient. A specific formulation can be derived to evaluate this component of the radiated sound field. The analytical development based on the work of Ffowcs-Williams & Mairanik¹⁹ has been extended in the spectral domain to get an expression for the acoustic power spectral density¹⁸.

$$S_{pp}(\mathbf{x}, \omega) = \frac{p_o^2}{32\pi^2 \rho_o} \quad (8)$$

$$\times \int_{V^*} \frac{\cos^2 \theta \sin^2 \theta}{C^5} \omega^2 G(\omega) \tau_t \delta_1^2 M_c dy$$

where δ_1 designates the mixing layer thickness and τ_t the typical turbulence time. The integration is performed over the volume V^* , defined as the set of points in the flow for which the convection Mach

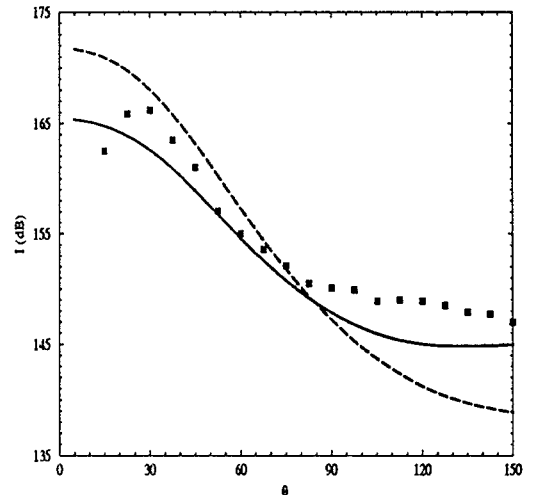


Figure 5: Directivity of a $M = 1.34$ jet as a function of the outlet angle θ . — Goldstein & Howes' model, ---- Ribner's model, ■ data of Tanna¹⁷ *et al.*

number exceeds unity. The function G is the Fourier transform of the pressure autocorrelation¹⁸:

$$G(\omega) = \left[1 - \frac{5}{8} \left(1 - \frac{\omega^2}{2\omega_M^2} \right) \right]$$

$$\times \frac{1}{2\sqrt{\pi}\omega_M} \exp\left(-\frac{\omega^2}{4\omega_M^2}\right)$$

where the angular frequency ω_M is given by $\omega_M = 2U_c^2 / (9\delta_1^2)$.

The peak spectral amplitude is plotted as a function of the observer angle θ in Figure 6. The predicted values are close to the experimental data of Seiner²⁴ *et al.* Other spectral comparisons with measurements and Tam's instability theory can be found in the literature.¹⁸ An example of spectral results is displayed in Figure 7 for a hot jet at $M = 2$. This figure shows that the Mach wave noise component of the radiated field is well represented.

As in previous models the acoustic intensity is obtained by an integration of the power spectral density over the angular frequency.¹⁸ An example of the resulting directivity is given in Figure 8 for a $M = 2$ free jet. The modeling provides only the Mach wave noise component, i.e. the directivity for the observer angle $\theta_M = \cos^{-1}(1/M_c)$. The mixing noise component evaluated by the two previous

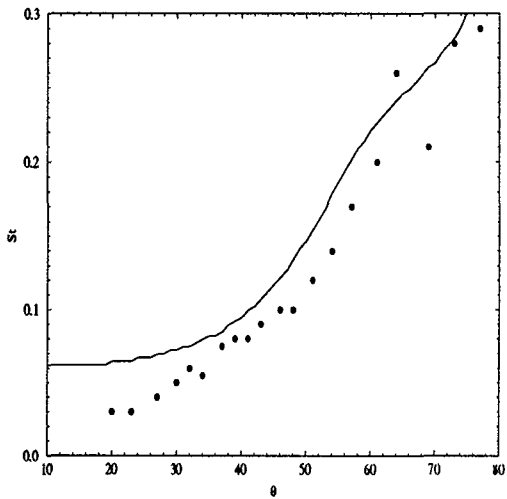


Figure 6: Comparison between the Mach wave noise model and experiments about the angular dependence of the peak spectral amplitude. — present Mach wave noise model, • data of Seiner²⁴ *et al.*. Round hot jet at $M = 2$ and $T_j/T_o = 2.5$

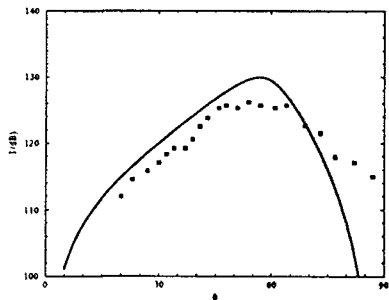
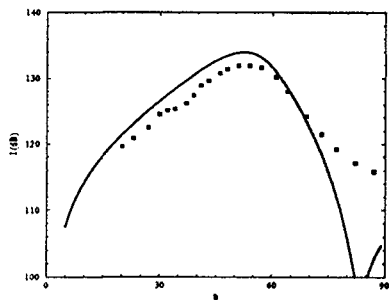
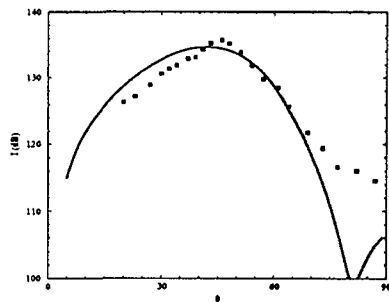
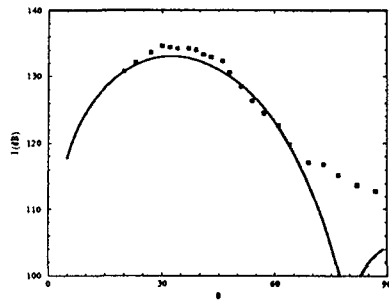


Figure 7: Mach wave noise component for 4 Strouhal numbers, $St = 0.05$, $St = 0.10$, $St = 0.20$, $St = 0.40$. Free round jet at $M = 2$ and $T_j/T_o = 2.5$. ■ data of Seiner²⁴ *et al.*

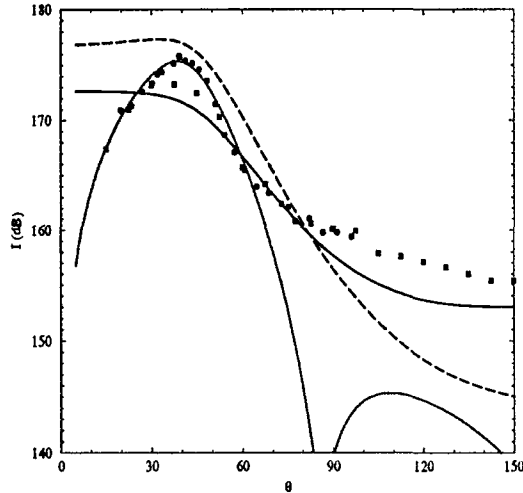


Figure 8: Directivity of a $M = 2$ and $T_j/T_o = 1$ jet. — mixing noise component with Goldstein & Howes' model, - - - mixing noise component with Ribner's model, - · - Mach wave noise component, • data of Seiner²⁴ *et al.* and ■ data of Tanna¹⁷ *et al.* with a $M = 1.95$ jet.

models is plotted too. Goldstein & Howes' theory more accurately predicts the experimental results in the upstream direction.

3. Application

As concluding remark Ribner's model (4) is applied to provide sound source localization. The power spectral density per unit length along the jet axis is defined as an integration across each section of the jet:

$$W_1(\mathbf{x}, y_1, \omega) = \int (S_a^{sf} + S_a^{sh}) dy_{\perp}$$

and the relative space-frequency distribution W_1/W_{1max} is plotted versus the dimensionless axial distance y_1/D and the Strouhal number St for a given observer angle $\theta = 90^\circ$. Figure 9 displays this representation of sound source localization with the hyperbolic time correlation (2) for a $M = 1.34$ cold, free, round jet. Generally, the high frequency sources are located in the mixing region near the nozzle while the low frequencies are situated in the downstream region. The predicted maximum is located at $y_1 \approx 6.4D$, i.e. near the end of the potential core $X_c \approx 8.4D$, with a Strouhal number $St \approx 0.25$.

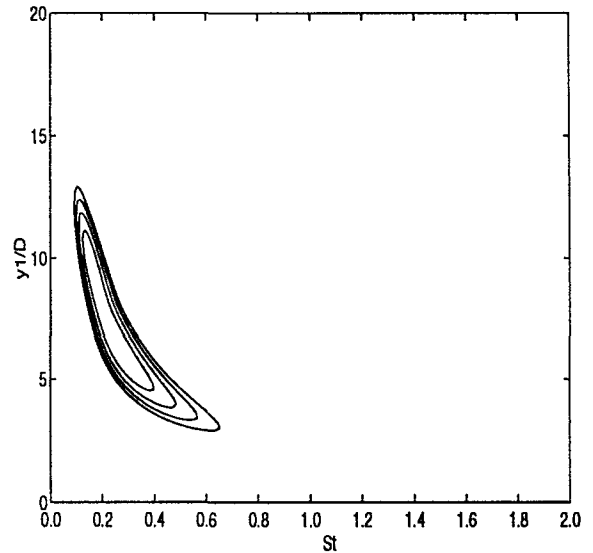


Figure 9: Relative power spectral density per unit length along the jet axis for an observer angle $\theta = 90^\circ$. Cold round, free, jet at $M = 1.34$. Ribner's model (3) with the hyperbolic time correlation (2). Four isolines from 0.8 to 0.95 with a step of 0.05.

To illustrate the influence of the time correlation function $g(\tau)$ in the model, the same representation is used in Figure 10 with a usual Gaussian time correlation in the power spectral density S_a (3). The maximum is located further downstream at $y_1 \approx 9.8D$ with a corresponding dimensionless frequency $St \approx 0.46$. This predicted Strouhal number is certainly too high in comparison with other studies.^{25,26}

With the model (4-2), the maximum of the spectral power density is plotted as a function of the dimensionless frequency St and the axial distance y_1/D in Figure 11. This numerical result is in agreement with the study of Dyer²⁵ based on a dimensional analysis.

Modeling using statistical turbulent sources can be an efficient tool for parametric studies of jet noise. In terms of sound source localization, the case of a $M = 2$ free jet has been investigated¹⁸ and comparison between experiments^{26,24} and numerical predictions shows good qualitative agreement. This approach has some limitations because of the necessary knowledge of the Green function for instance. To improve these models, refraction effects¹¹ and temperature sources should be taken into account.

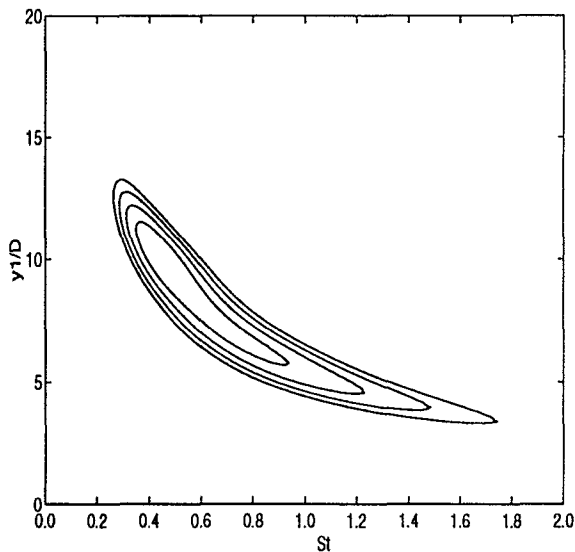


Figure 10: Relative power spectral density per unit length along the jet axis for an observer angle $\theta = 90^\circ$. Cold round, free, jet at $M = 1.34$. Ribner's model (3) with the usual Gaussian time correlation.¹⁴ Four isolines from 0.8 to 0.95 with a step of 0.05.

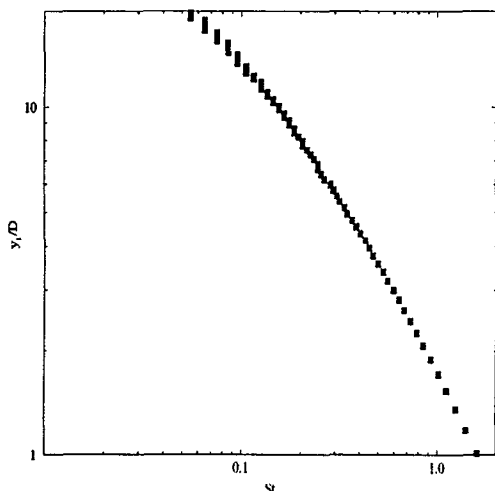


Figure 11: Maximum of the power spectral density as a function of the Strouhal number St and the dimensionless axial distance y_1/D . Cold round, free, jet at $M = 1.34$ for an observer angle $\theta = 90^\circ$.

Acknowledgments

I would like to thank Pr. G. Comte-Bellot and Pr. Daniel Juvé for fruitful discussions. Computing time was provided by Institut du Développement et des Ressources en Informatique Scientifique (IDRIS).

References

- ¹LIGHTHILL, M.J., 1952, On sound generated aerodynamically - I. General theory, *Proc. Roy. Soc. London*, **211**, A 1107, 564-587.
- ²LILLEY, G.M., 1991, Jet noise classical theory and experiments, in *Aeroacoustics of flight vehicles: theory and practice*, vol. 1: noise source, ed. H.H. Hubbard, *NASA Ref. Pub. 1258*, 211-289.
- ³TAM, C.K.W., 1995, Supersonic jet noise, *Ann. Rev. Fluid Mech.*, **27**, 17-43.
- ⁴TAM, C.K.W., 1995, Computational aeroacoustics: issues and methods, *AIAA Journal*, **33**(10), 1788-1796.
- ⁵LELE, S.K., 1997, Computational Aeroacoustics: a review, *35th Aerospace Sciences Meeting & Exhibit*, AIAA paper 97-0018.
- ⁶COMTE-BELLOT, G., BAILLY, C. & BLANC-BENON, P., 1997, Modelling tools for flow noise and sound propagation through turbulence, ed. O. Métais, Kluwer, 1-22, in press.
- ⁷WITKOWSKA, A., BRASSEUR, J.G. & JUVÉ, D., 1995, Numerical study of noise from stationary isotropic turbulence, *16th Aeroacoustics Conference*, AIAA paper 95-037.
- ⁸BASTIN, F., LAFON, P. & CANDEL, S., 1995, Computation of jet mixing noise from unsteady coherent structures, *16th Aeroacoustics Conference*, AIAA paper 95-039.
- ⁹BAILLY, C., LAFON, P. & CANDEL, S., 1995, A stochastic approach to compute noise generation and radiation of free turbulent flows, *16th AIAA Aeroacoustics Conference*, AIAA paper 95-092.
- ¹⁰BÉCHARA, W., LAFON, P., BAILLY, C. & CANDEL, S., 1995, Application of a $k - \epsilon$ model to the prediction of noise for simple and coaxial free jets, *J. Acoust. Soc. Am.*, **97**(6), 3518-3531.
- ¹¹KHAVARAN, A., KREJSA, E.A. & KIM, C.M., 1994, Computation of supersonic jet mixing noise for an axisymmetric convergent-divergent nozzle, *Journal of Aircraft*, **31**(3), 603-609.

- ¹²KHARAVAN, A., 1996, Refraction and shielding of noise in non-axisymmetric jets, *17th Aeroacoustic Conference*, AIAA Paper 96-1780.
- ¹³RIBNER, H.S., 1969, Quadrupole correlations governing the pattern of jet noise, *J. Fluid Mech.*, **38**(1), 1-24.
- ¹⁴BAILLY, C., LAFON, P. & CANDEL, S., 1994, Computation of subsonic and supersonic jet mixing noise using a modified $k - \epsilon$ model for compressible free shear flows, *Acta Acustica*, **2**(2), 110-112.
- ¹⁵BAILLY, C., BÉCHARA, W., LAFON, P. & CANDEL, S., 1993, Jet noise predictions using a $k - \epsilon$ turbulence model, *15th Aeroacoustics Conference*, AIAA Paper 93-4412.
- ¹⁶GOLDSTEIN, M.E. & HOWES, W.L., 1973, New aspects of subsonic aerodynamic noise theory, *National Aeronautics and Space Administration*, TN D-7158.
- ¹⁷TANNA, H.K., DEAN, P.D. & BURRIN, R.H., 1976, The generation and radiation of supersonic jet noise. Vol.III Turbulent mixing noise data, *Air Force Aero-Propulsion Laboratory, Lockheed-Georgia Company, Marietta*, AFAPL-TR-76-65.
- ¹⁸BAILLY, C., LAFON, P. & CANDEL, S., 1996, Prediction of supersonic jet noise from a statistical acoustic model and a compressible turbulence closure, *J. Sound Vib.*, **194**(2), 219-242.
- ¹⁹FFOWCS WILLIAMS, J.E. & MAIDANIK, G., 1965, The Mach wave field radiated by supersonic turbulent shear flows, *J. Fluid Mech.*, **21**(4), 641-657.
- ²⁰FFOWCS WILLIAMS, J.E., 1992, Noise source mechanisms, *Modern methods in analytical acoustics, lecture notes*, Springer-Verlag, 313-354.
- ²¹BATCHELOR, G.K., 1953, The theory of homogeneous turbulence, *Cambridge University Press*, Cambridge.
- ²²DAVIES, P.O.A.L., FISHER, M.J. & BARRATT, M.J., 1963, The characteristics of the turbulence in the mixing region of a round jet, *J. Fluid Mech.*, **15**(3), 337-367.
- ²³BAILLY, C., LAFON, P. & CANDEL, S., 1997, Subsonic and supersonic jet noise predictions from statistical source models, and a compressible turbulence closure, submitted to the *AIAA Journal*.
- ²⁴J. M. SEINER, M. K. PONTON, B. J. JANSEN & N. T. LAGEN, 1992, The effects of temperature on supersonic jet noise emission, *14th Aeroacoustics Conference*, AIAA paper 92-02-046.
- ²⁵DYER, I., 1959, Distribution of sound sources in a jet stream, *J. Acoust. Soc. Am.*, **31**(7), 1016-1022.
- ²⁶LAUFER, L., SCHLINKER, R. & KAPLAN, R.E., 1976, Experiments on supersonic jet noise, *AIAA Journal*, **14**(4), 489-497.